Monostatic Copolarized Simultaneous Transmit and Receive (STAR) Antenna by Integrated Single-Layer Design

Ziheng Zhou, Yue Li, *Senior Member, IEEE*, Jiadong Hu, Yijing He, Zhijun Zhang, *Fellow, IEEE*, and Pai-Yen Chen, *Senior Member, IEEE*

***Abstract*—In this letter, a monostatic and cochannel simultaneous transmit and receive (STAR) antenna with identical circularly polarized radiations of transmitting (TX) and receiving (RX) channels is designed using a thin single-layer substrate. Four concentrically arranged microstrip radiating elements are properly excited by two sets of feeding networks: the feeding network of transmitting antenna (FNT) and the feeding network of receiving antenna (FNR). To fit FNT and FNR into the same plane, the FNR consists of a compact sequential-phase structure placed at the center of the antenna, while the FNT is aligned along the side with a planar crossover junction armed. Two vital techniques, orthogonal feeding points and leakage signal cancellation based on feeding networks, are utilized for satisfactory isolation level between the TX and RX ports. The experiment results demonstrate an isolation at least 41 dB and up to 54 dB, an axial ratio better than 1.7 dB, and a realized gain of 7.2 $\sim$ 10.5 dBic in the 2.4 GHz WLAN band. Our design scheme may overcome the profile and cost limitations of bulky multilayered STAR antennas, and thus portends potential for the highly integrated inband duplex systems.**

***Index Terms*—Antenna array feed, circular polarization, monostatic, simultaneous transmit and receive (STAR) antennas, single layer.**

I. Introduction

THE inband duplex, or the so-called cochannel simultaneous transmit and receive (STAR) technique [1]–[3], has recently drawn great interest for its capability to double the throughput and reduce the time delay rate of communication systems. To effectively suppress the signal coupling between transmitting (TX) and receiving (RX) channels for STAR purpose, several stages of cancellation have to be considered, such as antennas, tunable analog circuits, and adaptive digital circuit cancellation layers [4], [5].

Manuscript received December 11, 2018; revised January 13, 2019; accepted January 17, 2019. Date of publication January 21, 2019; date of current version March 1, 2019. This work was supported in part by the National Natural Science Foundation of China under Grant 61771280, and in part by the Natural Science Foundation of Beijing Manipulate under Grant 4182029. *(Corresponding author: Yue Li.)*

Z. Zhou, Y. Li, J. Hu, Y. He, and Z. Zhang are with the Department of Electronic Engineering, Tsinghua University, Beijing 100084, China (e-mail: zhouzh17@mails.tsinghua.edu.cn; lyee@tsinghua.edu.cn; hjd17@mails.tsinghua.edu.cna; heyj16@mails.tsinghua.edu.cn; zjzh@tsinghua.edu.cn).

P.-Y. Chen is with the Department of Electrical and Computer Engineering, University of Illinois at Chicago, Chicago, IL 60607 USA (e-mail: pychen@uic.edu).

Digital Object Identifier 10.1109/LAWP.2019.2894418

To relieve the burden of subsequent circuit layers, traditional methods to enhance the isolation of the TX and RX ports of antenna layer involve bistatic antennas with large separation [3], [6], and the employment of circulators [7]–[11]. Electromagnetic bandgap structures [12], [13], resonators [14], and defected ground structures [15], arranged between TX and RX antennas, have also been proposed to suppress the signal interference in a narrow bandwidth. The near-field radiation pattern cancellation technique [16]–[19], polarization multiplexing [20]–[22], and the radiation pattern diversity [23] were alternatively used for the realization of good isolation, at the expense of different patterns and polarizations between TX and RX antennas.

Recently, a class of circularly polarized (CP) STAR antennas was proposed for the duplexing application, without any time-, space-, frequency-, or pattern-multiplexing [24]–[30]. In these works, the feeding networks of RX and TX antennas (FNR and FNT), with the strategically designed phase progress, can realize two functions simultaneously: 1) excitation of the far-field radiation with identical circular polarization, and 2) destructive superposition of the mutual coupling between TX and RX ports. In the previous works [24]–[30], multilayered configurations were used so that the antennas and feeding network can be designed independently on different layers, yet at the expense of expensive and bulky structure. In addition, assembling these systems usually requires air spacers to arrange the cables or the baluns for the feed, which could also increase the device profile.

Here, to address the above problems, we propose a low-profile, STAR antenna integrated with feeding networks on the same layer for applications in co-CP, co-channel, and co-pattern monostatic duplexing. In our approach, the FNR and FNT are properly tailored to excite four sequentially rotated square patches for realizing a broadside right-hand circularly polarized (RHCP) radiation. The FNR is strategically designed as a compact sequential phase feeding network (SPN) [31], [32] such that it can fit in the center space of the patch array. The FNT is arranged along the periphery of the array, with a planar crossover junction (PCJ) [33] introduced to address the intersection of microstrip lines. The isolation between two channels can be achieved by exciting orthogonal resonant modes in square patches [34], and further enhanced by two specifically designed feeding networks that cause destructive interference of

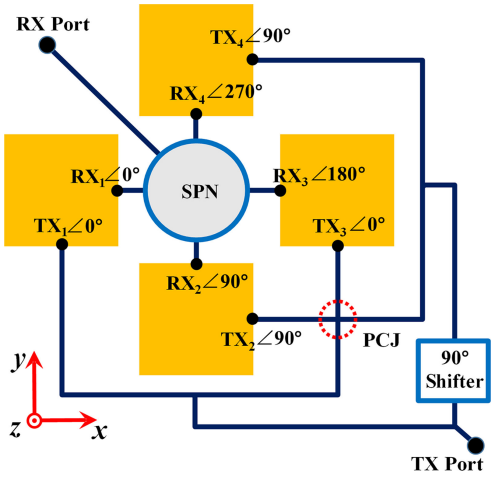

Fig. 1. Configuration of the proposed of single-layer co-CP STAR antenna integrated with the feeding networks. The planar crossover junction (PCJ) is denoted by the dashed circle.

couplings. We have prototyped the proposed single-layer STAR antenna operating in the 2.4 GHz WLAN band (2.4–2.48 GHz) with a size of 3.68 $\lambda_{\max}{}^2$ ($\lambda_{\max}$ is the free-space wavelength at 2.4 GHz). Both full-wave simulation and measurement results have demonstrated that a less than -10 dB reflection coefficient can be obtained for both ports and that the isolation can be higher than 41 dB over the band. Our results also show that the proposed STAR antenna can have good CP radiation performance, with a broadside axial ratio better than 1.7 dB and a RHCP gain higher than 7.2 dBic in the 2.4 GHz WLAN band.

II. Theory

The proposed scheme of the single-layer co-CP STAR antenna is illustrated in Fig. 1. Four square patches are sequentially rotated by 90° around the symmetry center, forming the radiation aperture. Each patch provides two orthogonal feeding points, RX_i and TX_i ($i = 1, 2, 3,$ and 4), that are connected to RX and TX channels. The main challenge for realizing single-layer co-CP STAR antenna resides in the design of FNR and FNT, simultaneously function as the co-CP feed and the leakage signal canceller.

To fit in the center space of the array with four square radiating patches and excite the CP radiation with wideband axial ratio, we use a SPN [31], [32] to construct the FNR, with a compact footprint of $\lambda/2 \times \lambda/2$. In this scheme, the four feeding points RX_1, RX_2, RX_3, and RX_4 are excited with the phase of 0°, 90°, 180°, and 270°, respectively, for generating a broadside RHCP beam.

The feeding network of TX antenna is basically built on a four-way power divider. The TX feeding points of the two oppositely placed patches are excited with equal phase and amplitude. Specifically, TX_1 and TX_3 are fed with the phase of 0°, while TX_2 and TX_4 are fed with the phase of 90°. As a result, the TX antenna also radiates toward broadside with the RHCP. The primary difficulty in the FNT design is the intersection of branches connecting TX_2 and TX_3. Here, a PCJ [33] is employed, which is denoted by the dashed circle in Fig. 1.

When the TX port is excited, the received signal at RX port is determined by the total contribution of leakage signals from RX_i ($i = 1, 2, 3,$ and 4) after considering the phase shift yielded by the FNR:

$$\mathrm{RX} = \mathrm{RX}_1\angle 0^\circ + \mathrm{RX}_2\angle 90^\circ + \mathrm{RX}_3\angle 180^\circ + \mathrm{RX}_4\angle 270^\circ. \tag{1}$$

For each term in the right-hand side of (1), the coupled signal at RX_i is contributed by the leakage signal from TX_j ($j = 1, 2, 3,$ and 4). For example, the coupling at RX_1 excited by TX port can be expressed as

$$\mathrm{RX}_1/TX = C_{11}\angle 0^\circ + C_{12}\angle 90^\circ + C_{13}\angle 0^\circ + C_{14}\angle 90^\circ \tag{2}$$

where the $C_{i,j}$ donates the transmission coefficient from TX_j to RX_i, and phase progress contributed by FNT has been taken into account in the summation. Substituting the expression of each RX_i into (1), the coupling signal from TX port to RX port can be written in a heuristic form through some manipulations

$$\mathrm{RX/TX} = \begin{bmatrix} \angle 0^\circ \\ \angle 90^\circ \\ \angle 180^\circ \\ \angle 270^\circ \end{bmatrix}^T \begin{bmatrix} C_{11} & C_{12} & C_{13} & C_{14} \\ C_{21} & C_{22} & C_{23} & C_{24} \\ C_{31} & C_{32} & C_{33} & C_{34} \\ C_{41} & C_{42} & C_{43} & C_{44} \end{bmatrix} \begin{bmatrix} \angle 0^\circ \\ \angle 90^\circ \\ \angle 0^\circ \\ \angle 90^\circ \end{bmatrix}. \tag{3}$$

The coupling mechanism in a matrix form offers an insight into the underlying physics. The coupling matrix $C_{i,j}$ is determined by the special arrangement of radiating elements, and the vectors multiplied at two sides depict the feeding phase progress of the FNR and FNT, respectively. By inspection to the symmetric layout (Fig. 1) of feed points TX_i and RX_i, we have the following constraints for the elements of coupling matrix:

$$C_{1,1} = C_{2,2} = C_{3,3} = C_{4,4} \tag{4a}$$

$$C_{2,1} = C_{2,3} = C_{3,4} = C_{3,2} \tag{4b}$$

$$C_{2,4} = C_{4,2} = C_{3,1} = C_{1,3} \tag{4c}$$

$$C_{1,4} = C_{1,2} = C_{4,1} = C_{4,3}. \tag{4d}$$

Imposing the above constraints to (3), the coupling between TX and RX ports vanishes. Although the scattering from the environment will introduce imbalance to the feeding phase and amplitude, our design still provides a high isolation level (for example, 40 dB).

III. Design and Test

To fulfill the design guidelines, a single-layer STAR antenna was characterized, fabricated, and measured at 2.4 GHz WLAN band (2.4–2.483 GHz). The antenna prototype is schematically shown in Fig. 2(a). The radiation aperture and the feeding networks are monolithically printed on a 2 mm dielectric substrate, with a relative dielectric constant of 2.2 and a loss tangent of 0.002. The center-to-center space D_p of the adjacent radiating elements is an important quantity to determine the performance of the STAR antenna. A too small D_p can lead to a stronger coupling among the radiating elements as well as the interference between radiating aperture and feeding networks, while an excessively large D_p will yield a radiation pattern with enhanced grating lobes and a reduced aperture efficiency. Hence,

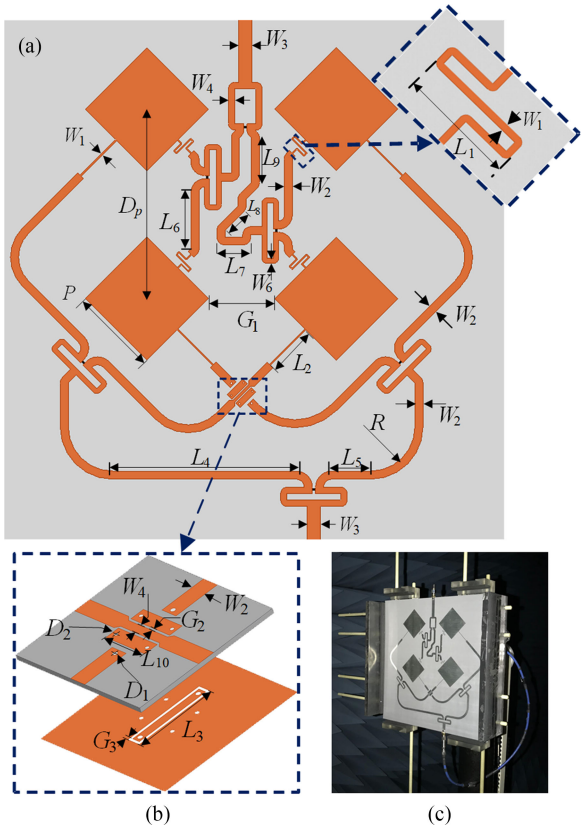

Fig. 2. (a) Schematic of designed single layer STAR antenna operating on 2.4 GHz WLAN band. The curve 1/4 λ impedance transformer is enlarged in the insets for clear vision. The critical parameters of the geometry are listed in Table I, and the lump resistors soldered in Wilkinson power dividers are with values of 130 Ω. (b) Planar crossover junction. (c) Photograph of the fabricated prototype.

a proper spacing distance ($0.65\lambda < D_p < 0.85\lambda$, for example) is needed. In this letter, the center-to-center space D_p of the adjacent patches is 84.8 mm (0.71λ at 2.5 GHz). The SPN is constructed in a quite miniaturized fashion, with a size of $\lambda/2 \times \lambda/2$ at the highest operating frequency (2.5 GHz). The impedance seen from the patch edge is 310 Ω. The λ/4 impedance transforming line (with the intrinsic impedance of 143 Ω) connected with the patches is arranged in a zigzag meander manner to further reduce the total area of the antenna. A miniaturized PCJ inspired by the work in [33] is designed for the layout of FNT. An enlarged perspective view of such a PCJ is shown in Fig. 2(b). The simulation of the PCJ showed that a reflection coefficient lower than −30 dB and an isolation better than 30 dB can be achieved for the intersected lines. The dimensions of the antenna and feeding networks were optimized using the Ansoft HFSS full-wave simulation. The total size of the antenna is 240 × 240 mm^2 (3.68 $\lambda_{max}{}^2$); detail design parameters are listed in Table I.

The fabricated co-CP single-layer STAR antenna by standard printed circuit board technique and the experiment setup are shown in Fig. 2(c). As can be seen in Fig. 3, a −14 dB reflection coefficient is obtained for each port over the frequency band of interest (2.4–2.5 GHz). The isolation tests were performed in two scenarios: a microwave anechoic chamber and a standard

TABLE I
DETAILED DIMENSIONS (UNIT: mm)

L_1	L_2	L_3	L_4	L_5	L_6	L_7	L_8	L_9
9.9	22.7	17	84	17.5	26.5	15.4	7.0	20.3
L_{10}	W_1	W_2	W_3	W_4	W_5	W_6	G_1	G_2
10	0.7	3.6	6.0	2.9	1.3	2.32	30.1	0.6
G_3	G_3	D_1	D_2	R	P	D_p		
1.0	3.0	1	0.8	20.8	39.5	84.8		

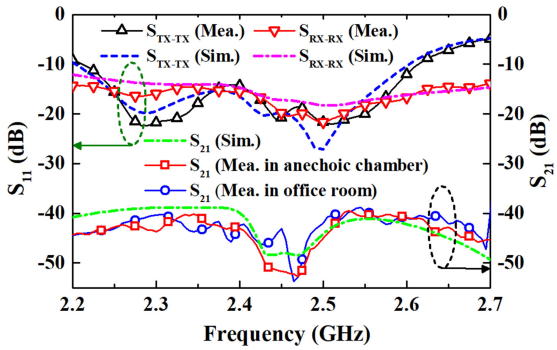

Fig. 3. Measured and simulated *S*-parameters of the TX and RX ports. The measurements of isolation are performed on two different conditions: in a microwave anechoic chamber and in a standard office room.

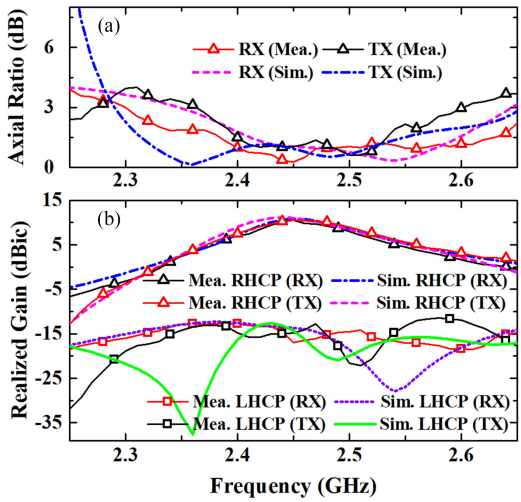

Fig. 4. (a) Simulated and measured broadside axial ratio of RX and TX antennas. (b) Simulated and measured broadside realized gain of RX and TX antennas.

office room exposed to the multipath interference. Fig. 3 presents the simulated and measured isolation between TX and RX ports, showing that a more than 41 dB insolation can be obtained from 2.4 to 2.5 GHz. Although being exposed to the multipath scattering environment, the 41 dB isolation can still be obtained in the frequency band of interest, demonstrating that our antenna is robust to the propagation channels.

The simulated and measured broadside axial ratio of TX and RX antennas are reported in Fig. 4(a), indicating that, for both RX and TX antennas, the axial ratio can be better than 1.7 dB from 2.4 to 2.5 GHz. The simulation and measurement results

TABLE II
COMPARISON OF OUR WORK WITH OTHER CO-CHANNEL CO-CP STAR ANTENNAS

Ref.	Operating band (GHz)	Isolation	Realized Gain	Axial Ratio	Multilayer/ Single-layer	Peak aperture efficiency	Size	Total Profile	Cost
[24]	2.4-2.5	>47 dB	7-10.8 dBic	<1.6 dB	Multilayer	31.0%	2.56 λ_{max}^2	0.037 λ_{max}[a]	High
[25]	6.0-7.2	>40 dB	8.7-12.5 dBic	<3 dB	Multilayer	16.4%	4.84 λ_{max}^2	0.073 λ_{max}[b]	High
[26]	0.65-2.75	>27 dB	2-13 dBic	<4.3 dB	Multilayer	29.9%	0.66 λ_{max}^2	0.065 λ_{max}	High
[27]	5.4-5.6	>33 dB	6 dBic	< 2 dB	Multilayer	29.5%	1.08 λ_{max}^2	0.014 λ_{max}	High
[28]	0.9-0.92	>40 dB	1 dBic	< 2 dB	Multilayer	49.8%	0.151λ_{max}^2	0.089 λ_{max}	High
This work	2.4-2.5	>41 dB	7.2-10.5 dBic	<1.7 dB	Single-layer	22.4%	3.68 λ_{max}^2	0.016 λ_{max}	Reduced by half and more[c]

[a]The thickness of the air spacer to arrange the cables is not included.

[b]The profile of the feeding network fixture is not included.

[c]Compared with multilayer structures, the single-layer scheme can reduce the cost by half and even more.

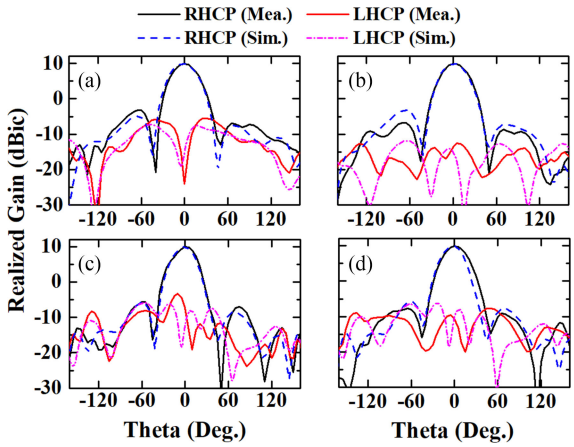

Fig. 5. Simulated and measured realized gain of RX and TX antennas versus elevation angle at 2.45 GHz. (a) Patterns of RX antenna on *x*–*z* cut plane. (b) Patterns of RX antenna on *y*–*z* cut plane. (c) Patterns of TX antenna on *x*–*z* cut plane. (d) Patterns of TX antenna on *y*–*z* cut plane.

are in good agreement. The measured broadside realized gain of RX and TX antennas are reported in Fig. 4(b), respectively. The results show that the both RX and TX antennas can offer a maximum RHCP gain of ∼10.5 dBic and a 3 dB gain variation bandwidth from 2.4 to 2.5 GHz. The cross-polarization level is lower than −21 dB within the band of interest.

Fig. 5 reports the simulated and measured realized gain of RX and TX antennas versus elevation angle at 2.45 GHz on the *x*–*z* and *y*–*z* cut planes. The simulation (measurement) result shows a 15.5 dB (14.1 dB) cross-polarization rejection, corresponding to the 3 dB (3.5 dB) axial ratio within the half-power beamwidth. In addition, the RX and TX antennas show similar broadside patterns, verifying that the proposed inband duplex scheme does not require any polarization or pattern multiplex. We also measured the total efficiency of TX and RX antennas considering the feeding networks, with the peak efficiencies of ∼80% being obtained.

In Table II, we compare results presented in this letter with the state-of-the-art co-channel co-CP STAR antennas. As seen, the proposed single-layer co-CP STAR antenna not only exhibits a good CP performance and a high isolation between the RX and TX ports, but also provides advantages like low profile, low cost, and good integrability with planar circuits. We note that, for fair comparison, the physical size of the single-layer antenna considers also the area of feeding networks, which makes the aperture efficiency of the proposed antenna relatively lower. This aspect can be further improved by using more compact feeding networks and optimizing the antenna shape.

IV. CONCLUSION

In this letter, we propose a co-CP STAR antenna based on single-layer architecture, realizing the integration of complex feeding networks and the radiation aperture in the same layer. Both full-wave simulation and measurement results show that the proposed STAR antenna can offer an insolation higher than 41 dB in the whole 2.4 GHz WLAN band (2.4–2.5 GHz). For both TX and RX antennas, robust CP performance is obtained, with an axial ratio better than 1.7 dB and a RHCP realized gain of 7.2 ∼10.5 dBic in the operating band. We envision that the proposed single-layer STAR antenna, with advantages over the traditional multilayer schemes like eased integration, low cost, and extreme thinness, may impact duplexing systems in the forthcoming 5G communication.

REFERENCES

[1] A. Sabharwal, P. Schniter, D. Guo, D. W. Bliss, S. Rangarajan, and R. Wichman, "In-band full-duplex wireless: Challenges and opportunities," *IEEE J. Sel. Areas Commun.*, vol. 32, no. 9, pp. 1637–1652, Sep. 2014.

[2] T. Snow, C. Fulton, and W. J. Chappell, "Transmit-receive duplexing using digital beamforming system to cancel self-interference," *IEEE Trans. Microw. Theory Techn.*, vol. 59, no. 12, pp. 3494–3503, Dec. 2011.

[3] J. I. Choi, M. Jain, K. Srinivasan, P. Levis, and S. Katti, "Achieving single channel full duplex wireless communications," in *Proc. 16th Annu. Int. Conf. Mobile Comput. Netw.*, 2010, pp. 1–12.

[4] Z. Zhang, X. Chai, K. Long, A. V. Vasilakos, and L. Hanzo, "Full duplex techniques for 5G networks: Self-interference cancellation, protocol design, and relay selection," *IEEE Commun. Mag.*, vol. 53, no. 5, pp. 128–137, May 2015.

[5] A. Goldsmith, *Wireless Communications*. New York, NY, USA: Cambridge Univ. Press, 2005.

[6] P. V. Prasannakumar, M. A. Elmansouri, and D. S. Filipović, "Wideband decoupling techniques for dual-polarized bi-static simultaneous transmit and receive antenna subsystem," *IEEE Trans. Antennas Propag.*, vol. 65, no. 10, pp. 4991–5001, Oct. 2017.

[7] S. L. Karode and V. F. Fusco, "Feedforward embedding circulator enhancement in transmit/receive applications," *IEEE Microw. Guided Wave Lett.*, vol. 8, no. 1, pp. 33–34, Jan. 1998.

[8] D. Bharadia, E. McMilin, and S. Katti, "Full duplex radios," *ACM SIGCOMM Comput. Commun. Rev.*, vol. 43, no. 4, pp. 375–386, Oct. 2013.

[9] C. H. Cox and E. I. Ackerman, "Photonics for simultaneous transmit and receive," in *IEEE Microw. Symp. Dig.*, Baltimore, MD, USA, Jun. 2011, pp. 1–4.
[10] N. A. Estep, D. L. Sounas, and A. Alù, "Magnetless microwave circulators based on spatiotemporally modulated rings of coupled resonators," *IEEE Trans. Microw. Theory Techn.*, vol. 64, no. 2, pp. 502–518, Feb. 2016.
[11] A. Kord, D. L. Sounas, and A. Alù, "Magnet-less circulators based on spatiotemporal modulation of bandstop filters in a delta topology," *IEEE Trans. Microw. Theory Techn.*, vol. 66, no. 2, pp. 911–926, Feb. 2018.
[12] L. Yang, M. Fan, F. Chen, J. She, and Z. Feng, "A novel compact electromagnetic-bandgap (EBG) structure and its applications for microwave circuits," *IEEE Trans. Microw. Theory Techn.*, vol. 53, no. 1, pp. 183–190, Jan. 2005.
[13] F. Yang and Y. Rahmat-Samii, "Microstrip antennas integrated with electromagnetic band-gap (EBG) structures: A low mutual coupling design for array applications," *IEEE Trans. Antennas Propag.*, vol. 51, no. 10, pp. 2936–2946, Oct. 2003.
[14] A. T. Wegener and W. J. Chappell, "Simultaneous transmit and receive with a small planar array," in *IEEE MTT-S Int. Microw. Symp. Dig.*, Montreal, QC, Canada, Jun. 2012, pp. 1–3.
[15] G. Makar, N. Tran, and T. Karacolak, "A high isolation monopole array with ring hybrid feeding structure for in-band full-duplex systems," *IEEE Antennas Wireless Propag. Lett.*, vol. 16, pp. 356–359, 2017.
[16] K. E. Kolodziej, P. T. Hurst, A. J. Fenn, and L. I. Parad, "Ring array antenna with optimized beamformer for simultaneous transmit and receive," in *Proc. IEEE Int. Symp. Antennas Propag.*, Chicago, IL, USA, Jul. 2012, pp. 1–2.
[17] W. F. Moulder, B. T. Perry, and J. S. Herd, "Wideband antenna array for simultaneous transmit and receive (STAR) applications," in *Proc. IEEE Int. Symp. Antennas Propag.*, Memphis, TN, USA, Jul. 2014, pp. 243–244.
[18] R. Lian, T. Y. Yin, Y. Yin, and N. Behdad, "A high-isolation, ultra-wideband simultaneous transmit and receive antenna with monopole-like radiation characteristics," *IEEE Trans. Antennas Propag.*, vol. 66, no. 2, pp. 1002–1007, Feb. 2018.
[19] W. J. Kaminski, "Simultaneous transmit and receive antenna," U.S. Patent 5038151, Aug. 1991.
[20] E. Yetisir, C. C. Chen, and J. L. Volakis, "Wideband low profile multiport antenna with omnidirectional pattern and high isolation," *IEEE Trans. Antennas Propag.*, vol. 64, no. 9, pp. 3777–3786, Sep. 2016.
[21] A. Batgerel and S. Y. Eom, "High-isolation microstrip patch array antenna for single channel full duplex communications," *Microw., Antennas Propag.*, vol. 9, no. 11, pp. 1113–1119, Aug. 2015.
[22] E. Everett, A. Sahai, and A. Sabharwal, "Passive self-interference suppression for full-duplex infrastructure nodes," *IEEE Trans. Wireless Commun.*, vol. 13, no. 2, pp. 680–694, Jan. 2014.
[23] T. Snow, C. Fulton, and W. J. Chappell, "Multi-antenna near field cancellation duplexing for concurrent transmit and receive," in *Proc. IEEE MTT-S Int. Microw. Symp.*, Baltimore, MD, USA, 2011, pp. 1–4.
[24] J. Ha, M. A. Elmansouri, P. V. Prasannakumar, and D. S. Filipović, "Monostatic co-polarized full-duplex antenna with left or right hand circular polarization," *IEEE Trans. Antennas Propag.*, vol. 65, no. 10, pp. 5103–5111, Oct. 2017.
[25] J. Wu, M. Li, and N. Behdad, "A wideband, unidirectional circularly polarized antenna for full-duplex applications," *IEEE Trans. Antennas Propag.*, vol. 66, no. 3, pp. 1559–1563, Mar. 2018.
[26] M. A. Elmansouri, A. J. Kee, and D. S. Filipović, "Wideband antenna array for simultaneous transmit and receive (STAR) applications," *IEEE Antennas Wireless Propag. Lett.*, vol. 16, pp. 1277–1280, 2017.
[27] H. S. Jang, W. G. Lim, W. I. Son, S. Y. Cha, and J. W. Yu, "Microstrip patch array antenna with high isolation characteristics," *Microw. Opt. Technol. Lett.*, vol. 54, no. 4, pp. 973–976, Apr. 2012.
[28] W. G. Lim, W. I. Son, K. S. Oh, W. K. Kim, and J. W. Yu, "Compact integrated antenna with circulator for UHF RFID system," *IEEE Antennas Wireless Propag. Lett.*, vol. 7, pp. 673–675, 2008.
[29] E. A. Etellisi, M. A. Elmansouri, and D. S. Filipović, "In-band full-duplex multimode lens-loaded eight-arm spiral antenna," *IEEE Trans. Antennas Propag.*, vol. 66, no. 4, pp. 2084–2089, Apr. 2018.
[30] E. A. Etellisi, M. A. Elmansouri, and D. S. Filipović, "Wideband monostatic simultaneous transmit and receive (STAR) antenna," *IEEE Trans. Antennas Propag.*, vol. 64, no. 1, pp. 6–15, Jan. 2016.
[31] S. Lin and Y. Lin, "A compact sequential-phase feed using uniform transmission lines for circularly polarized sequential-rotation arrays," *IEEE Trans. Antennas Propag.*, vol. 59, no. 7, pp. 2721–2724, Jul. 2011.
[32] C. Deng, Y. Li, Z. Zhang, and Z. Feng, "A wideband isotropic radiated planar antenna using sequential rotated L-shaped monopoles," *IEEE Trans. Antennas Propag.*, vol. 62, no. 3, pp. 1461–1464, Mar. 2014.
[33] W. Liu, Z. Zhang, Z. Feng, and M. Iskander, "A compact wideband microstrip crossover," *IEEE Microw. Wireless Compon. Lett.*, vol. 22, no. 5, pp. 254–256, May 2012.
[34] M. J. Cryan, P. S. Hall, S. H. Tsang, and J. Sha, "Integrated active antenna with full duplex operation," *IEEE Trans. Microw. Theory Techn.*, vol. 45, no. 10, pp. 1742–1748, Oct. 1997.